We are IntechOpen,
the world's leading publisher of
Open Access books
Built by scientists, for scientists

4,800
Open access books available

122,000
International authors and editors

135M
Downloads

Our authors are among the

154
Countries delivered to

TOP 1%
most cited scientists

12.2%
Contributors from top 500 universities

CLARIVATE ANALYTICS
BOOK CITATION INDEX
INDEXED

WEB OF SCIENCE™

Selection of our books indexed in the Book Citation Index
in Web of Science™ Core Collection (BKCI)

Interested in publishing with us?
Contact book.department@intechopen.com

Numbers displayed above are based on latest data collected.
For more information visit www.intechopen.com

A Hybrid Energy Storage System for a Coaxial Power-Split Hybrid Powertrain

Enhua Wang, Fuyuan Yang and Minggao Ouyang

Additional information is available at the end of the chapter

Abstract

A hybrid energy storage system (HESS) consisting of batteries and supercapacitors can be used to reduce battery stress and recover braking energy efficiently. In this paper, the performance of a novel coaxial power-split hybrid transit bus with an HESS is studied. The coaxial power-split hybrid powertrain consists of a diesel engine, a generator, a clutch, and a motor, whose axles are arranged in a line. A mathematical model of the coaxial power-split hybrid powertrain with an HESS is established and the parameters are configured using experimental data. Subsequently, to estimate the system performance, a program is designed based on Matlab and Advisor. A rule-based control strategy is designed and finely tuned for the coaxial power-split hybrid powertrain. Then, using the Chinese Transit Bus City Driving Cycle (CTBCDC), the system characteristics and energy efficiencies of the designed coaxial power-split hybrid powertrain with an HESS are analysed. The results indicate that the proposed coaxial power-split hybrid powertrain with an HESS can fulfil the drivability requirement of transit bus and enhance the energy efficiency significantly compared with a conventional powertrain bus as well as reduce the battery stress simultaneously. Using an HESS is a good solution for the coaxial power-split hybrid transit bus.

Keywords: coaxial power-split hybrid electric bus, hybrid energy storage system, supercapacitor, lithium-ion battery, performance simulation

1. Introduction

Energy conservation and emission reduction are two important tasks for a sustainable development of our industrial society. In terms of automotive industry, applications of hybrid electric

vehicle (HEV), electric vehicle (EV), and fuel cell vehicle (FCV) are effective technical approaches for energy conservation and emission reduction [1, 2]. Currently, EV and HEV cannot comprehensively fulfill the requirements of transit buses due to their poor durability and high cost. However, HEV is a feasible solution with high reliability and relatively low cost.

There are two kinds of power source for an HEV: one is internal combustion engine, and the other is electric energy storage system (ESS). An ESS can discharge electric power to propel the vehicle or absorb electric power during the regenerative braking process. Generally, the architecture of an HEV powertrain can be classified as series hybrid, parallel hybrid, and power-split hybrid [3]. Taking into account the heavy-duty hybrid powertrain for transit buses, series hybrid and parallel hybrid are widely adopted presently. For instance, Orion VII and Man Lion use series hybrid powertrain for their transit buses. Volvo and Eaton designed two types of parallel hybrid powertrain for heavy-duty applications.

With the progress of technology, the battery used for the ESS of an HEV has been gradually shifted from lead-acid, NiCad, and Ni-MH to lithium-ion battery. Lithium-ion batteries will be used widely as the ESS for various vehicles because of their high-energy density, good safety, and long durability [4]. Currently, the materials of lithium-ion batteries are mainly lithium iron phosphate and nickel-cobalt-manganese ternary composite [5]. An HEV transit bus undergoes frequent acceleration and deceleration during its working time and requires large working currents of the ESS for these processes. Because the discharge and charge rates of lithium-ion battery are limited, if the ESS consists of only lithium-ion batteries, a large capacity of lithium-ion batteries is required, which will increase the cost and weight of an HEV greatly. To overcome this problem, hybrid energy storage system (HESS) composed of lithium-ion batteries and supercapacitors is employed. In contrast to a lithium-ion battery, a supercapacitor can charge or discharge with very large instantaneous currents. This characteristic can provide sufficient electric power during the acceleration process and store electric energy during the regenerative braking process. Because supercapacitors use a porous carbon-based electrode material, a very high effective surface area can be obtained by this porous structure compared to a conventional plate structure. Supercapacitors also have a minimal distance between the electrodes, which result in a very high capacitance compared to a conventional electrolytic capacitor [6, 7]. Apart from the fast charge/discharge rates and the high-power density, supercapacitors have much longer lifetimes (>100,000 cycles) compared to lithium-ion batteries [8–10]. However, supercapacitors normally have a much smaller energy capacity compared with lithium-ion batteries. Therefore, using an HESS can fully utilize the advantages of these two kinds of energy storage devices and avoid their disadvantages.

Figure 1 shows four primary topologies of an HESS, which encompass passive hybrid topology, supercapacitor semi-active hybrid topology, battery semi-active hybrid topology, and parallel active hybrid topology [11, 12]. The passive hybrid topology is the simplest to combine battery and supercapacitor together. The advantage of this topology is that no power electronic converters are needed. Because the voltage of the DC bus is stabilized by the battery, the stored energy of the supercapacitor cannot be utilized sufficiently. In the supercapacitor semi-active topology, the battery is connected to the DC bus directly, while the supercapacitor uses a bidirectional DC/DC converter to interface the DC bus. As a result, the voltage of the DC bus equals the output voltage of the battery so that it cannot be varied too much. But the voltage of the supercapacitor can be changed in a wide range. The disadvantage of this topology is that a large size of DC/DC converter
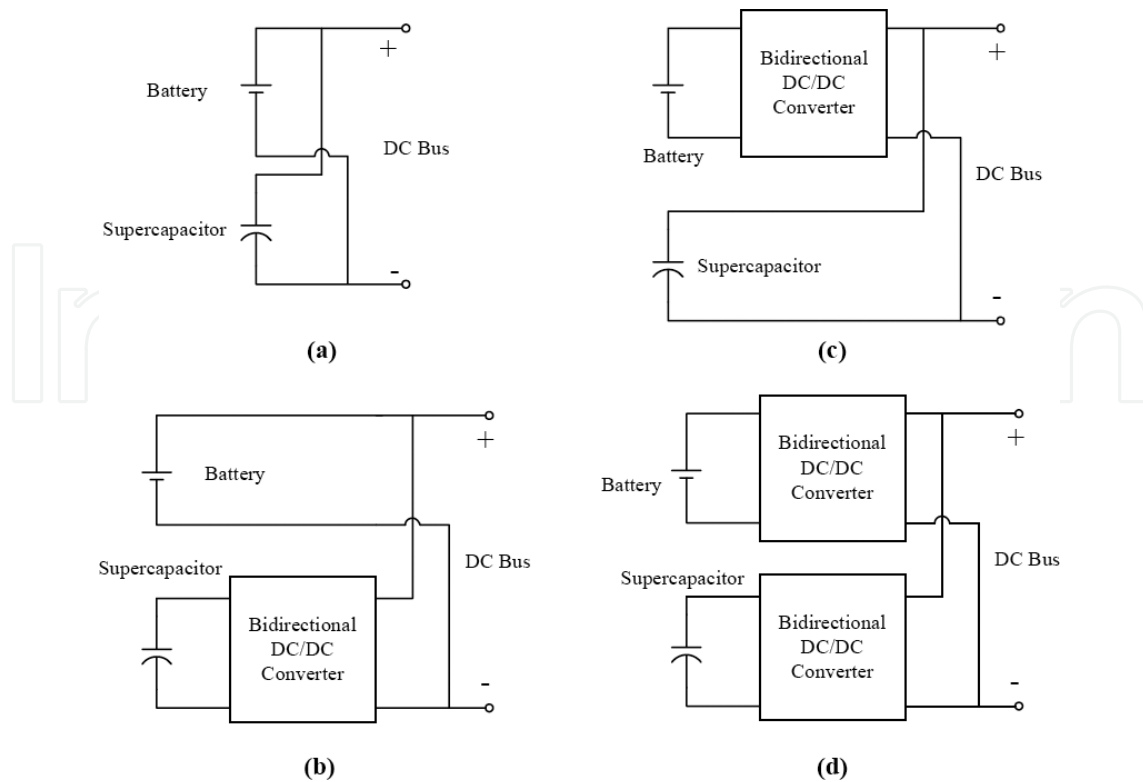
Figure 1. Topologies of hybrid energy storage system for vehicle application: (a) passive hybrid topology, (b) supercapacitor semi-active hybrid topology, (c) battery semi-active hybrid topology, and (d) parallel active hybrid topology.

is required. In the battery semi-active topology, the supercapacitor is connected to the DC bus directly, while the battery uses a bidirectional DC/DC converter to interface the DC bus. The advantage is the battery current can be maintained at a near constant value, thus the lifetime and energy efficiency of the battery can be improved significantly. The main shortcoming of this topology is that the voltage of the DC bus will vary during the charging/discharging process of the supercapacitor. The parallel hybrid topology is an optimal choice that can solve all the problems of the above topologies. The disadvantage is that two DC/DC converters are needed which will increase complexity, cost, and additional losses of the system. Three different topologies of HESS using supercapacitors as the main energy storage device for EV application were analyzed by Song et al. [13]. Rothgang et al. studied the performance of an active hybrid topology [14]. Among these various architectures, the supercapacitor semi-active hybrid topology using lithium-ion batteries as the main storage device is considered as a good solution for HEV application due to its high-power density and low cost.

Most of investigations about HESS focus on EV applications. Hung and Wu designed a rule-based control strategy for the HESS of an EV and estimated the system performance [15]. Vulturescu et al. tested the performance of an HESS consisting of NiCad batteries and supercapacitors [16]. Song et al. compared three different control strategies for an HESS, which included a rule-based control, a model predictive control, and a fuzzy logic control [17]. An HESS can also be used with a fuel cell and successfully satisfy the requirements of an FCV [18–20]. However, few investigations are concentrated on the application of an HESS for an HEV at present because they are more complicated than those for an EV. Masih-Tehrani et al. studied the energy management

strategy of an HESS for a series hybrid powertrain [21] and Nguyen et al. investigated the performance of a belt-driven starter generator (BSG)-type parallel hybrid system with an HESS [22]. All these studies give the HESS an advantage over the ESS with only batteries.

The control strategy of an HESS for an EV is easier than that for an HEV or an FCV because it only needs to consider the power distribution between the batteries and supercapacitors. By contrast, the control strategy of an HEV with an HESS must assign the power demand of vehicle among the ICE, the batteries, and the supercapacitors, thus it is more complicated. Currently, few researches about the HESS for a power-split HEV are reported. In this study, a coaxial power-split HEV with an HESS for heavy-duty transit bus application is evaluated. The HESS uses lithium-ion batteries as the main energy storage device. The performance of the hybrid transit bus is analyzed using the Chinese Transit Bus City Driving Cycle (CTBCDC).

2. System description

Figure 2 shows the architecture of the designed coaxial power-split hybrid powertrain for a transit bus with a supercapacitor semi-active hybrid energy storage system. The auxiliary power unit (APU) consists of a diesel engine and a permanent magnetic synchronous generator (PMSG)
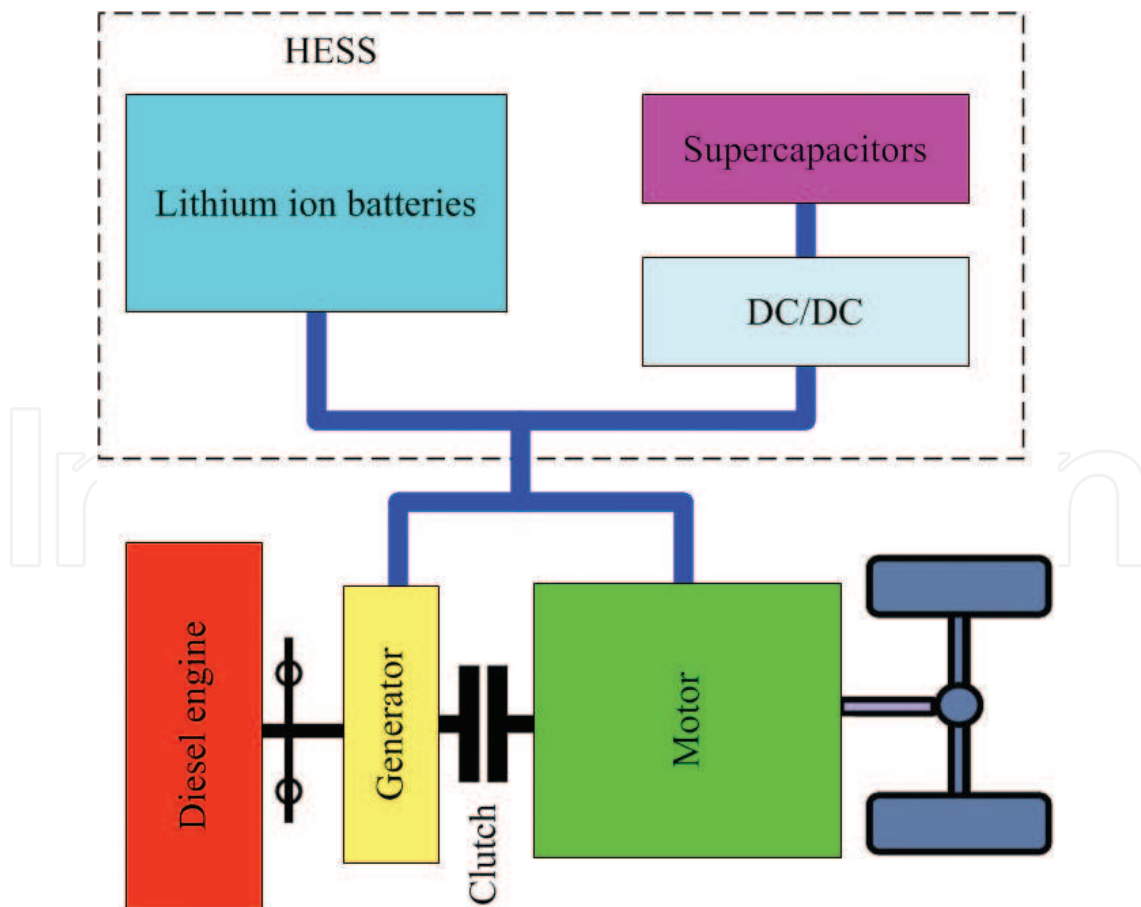
Figure 2. Architecture of the designed coaxial power-split hybrid powertrain with a hybrid energy storage system for transit bus where a CNG engine, a generator, a clutch, and a motor are arranged sequentially in a line.

whose shafts are connected directly. This shaft is also associated with the input axle of the clutch. The output axle of the clutch is linked to a permanent magnetic synchronous motor (PMSM) whose shaft is also connected to the final drive. Besides the diesel engine, an HESS composed of lithium-ion batteries and supercapacitors as well as a bidirectional DC/DC converter is used to provide electric power to the PMSM. A high-voltage power line is connected to the PMSG, the PMSM, the battery pack, and the DC/DC converter. The supercapacitor pack exchanges electric power with the high-voltage power line via the controllable bidirectional DC/DC converter.

The main technical parameters of the designed coaxial power-split hybrid powertrain with an HESS are listed in **Table 1**. The internal combustion engine is a 6.5 L YC6J220 diesel engine manufactured by Yuchai Machinery Co., Ltd. The supercapacitor pack is composed serially of 12 units of Maxwell 48-V module. The battery pack consists of nine paralleled groups and each

Component	Parameter	Value	Unit
Engine	Type	YC6J220 diesel engine	–
	Rated power	162	kW
	Rated speed	2500	r/min
	Maximum torque	760	N·m
	Peak efficiency	41.9	%
Supercapacitors	Type	Maxwell 48-V module	–
	Number of modules	12	–
	Energy capacity	0.651	kWh
	Rated voltage	576	V
	Voltage range	172–570	V
Batteries	Type	A123 26650 LiFePO$_4$ cell	–
	Number of modules	1701	–
	Energy capacity	14	kWh
	Rated voltage	604	V
	Voltage range	570–591	V
Motor	Type	Jing-Jin Electric PMSM	–
	Rated power	150	kW
	Rated speed	3000	r/min
	Maximum torque	2100	N·m
	Peak efficiency	93.5	%
Generator	Type	Jing-Jin Electric PMSG	–
	Rated power	135	kW
	Rated speed	3000	r/min
	Maximum torque	850	N·m
	Peak efficiency	94.5	%

Table 1. Technical specifications of the coaxial power-split hybrid powertrain.

group is serially connected by 189 cells of the A123 nanophosphate lithium-ion ANR26650M1-B cell. The energy capacity of the battery pack is decided by the all-electric driving range, and its c-rate is defined by the average output power. In this design, the energy capacity of the battery pack is 14 kWh. Both the PMSG and the PMSM are low-speed high-power electric machines developed by Jing-Jin Electric Technologies Co., Ltd.

3. Mathematical model

A mathematical model of the coaxial power-split hybrid powertrain with an HESS is established to analyze the system performance. According to the working principle of the entire system, a lumped-parameter model is used.

3.1. Vehicle dynamics

Since the rear axle is used to drive the hybrid transit bus, the tractive force of the rear axle is determined according to the longitudinal vehicle dynamics [23].

$$\mathrm{F} = \mathrm{F}_r + \mathrm{F}_a + \mathrm{F}_i + \mathrm{F}_j = mg\cos\alpha(f_1 + f_2 v) + \frac{1}{2}\rho A C_D v_r^2 + mg\sin\alpha + \delta m\frac{dv}{dt} \tag{1}$$

Therefore, the tractive force F can be calculated according to the practical driving conditions.

The loads of the front and rear axles can be calculated based on the vehicle parameters. Then, the friction factor and the slip of the tires can be determined due to the required tractive force and the axle load. Moreover, the rotating speed and the driving torque of the tires can be obtained. If the vehicle is braking, the braking force imposed on the rear axle can be computed according to the braking force distribution equation. Then, the braking torque and speed of the rear tires can be determined. Subsequently, the model of the final drive determines the rotating speed ω_m and the torque T_m taking into account the friction loss T_{l0} and the rotating inertia J_0.

$$\mathrm{T}_m = \frac{T_w}{i_0} + T_{l0} + i_0 J_0 \frac{d\omega}{dt} \tag{2}$$

$$\omega_m = i_0\omega \tag{3}$$

The PMSM model accounts for the requested torque T_{mr} and the input power P_m calculated by a two-dimensional (2D) lookup table measured from a motor test bench [24].

In the coaxial power-split hybrid powertrain, a clutch is used to control the operation mode that is either the series or the parallel mode. The mathematical model of the clutch is a simple friction model [25], which is used to determine the clutch state among the engaged, the slipping, and the disengaged states. The torque and speed transmitted through the clutch are also determined.

3.2. Auxiliary power unit

Normally, an auxiliary power unit is a combination of the engine and the generator. The diesel engine model accounts for the requested torque T_{er} according to the engine output torque T_e and the engine speed ω_e.

$$T_{er} = T_e + J_e \frac{d\omega_e}{dt} \tag{4}$$

Subsequently, the fuel consumption M_e is calculated using the density of diesel fuel ρ_f for the diesel engine.

$$M_e = \frac{\displaystyle\int_0^{t_c} m_e dt}{\rho_f \displaystyle\int_0^{t_c} v dt} \tag{5}$$

where t_c is the final time of the driving cycle. The mathematical model of the generator is similar with the motor. The requested torque T_{gr} is determined according to the input torque of the generator T_g and the inertia J_g. The output power P_g is a function of the generator speed ω_g and torque T_{gr} defined by a 2D lookup table.

$$T_{gr} = T_g + J_g \frac{d\omega_g}{dt} \tag{6}$$

$$P_g = f(\omega_g, T_{gr}) \tag{7}$$

3.3. Hybrid energy storage system

The model of lithium-ion batteries of the designed HESS is a *Rint* model [24]. If the output power of the battery pack is P_{bat}, the energy equilibrium of this circuit can be expressed as

$$R_{\mathrm{bat}} i_{\mathrm{bat}}^2 - U_{\mathrm{bat}} i_{\mathrm{bat}} + P_{\mathrm{bat}} = 0 \tag{8}$$

Then, the current of the battery is calculated by

$$i_{\mathrm{bat}} = \frac{U_{\mathrm{bat}} - \sqrt{U_{\mathrm{bat}}^2 - 4R_{\mathrm{bat}} P_{\mathrm{bat}}}}{2R_{\mathrm{bat}}} \tag{9}$$

The *SOC* of the lithium-ion batteries at time k is defined as

$$SOC_{\mathrm{bat},k} = SOC_{\mathrm{bat},0} + \int_{t=0}^{k} i_{\mathrm{bat}}(t)dt \tag{10}$$

The internal resistance R_{bat} and capacitance C_{bat} are calculated via looking up two 2D maps. The data of these maps are obtained according to the references [26, 27] for A123 system's ANR26650M1-B lithium-ion battery.

The supercapacitors of the designed HESS use an *RC* model [24]. Given the output power of the supercapacitors P_{sc}, the energy equation of the supercapacitor circuit is expressed as

$$R_{sc}i_{sc}^2 - U_{sc}i_{sc} + P_{sc} = 0 \tag{11}$$

Then, the current of the supercapacitors is obtained by

$$i_{sc} = \frac{U_{sc} - \sqrt{U_{sc}^2 - 4R_{sc}P_{sc}}}{2R_{sc}} \tag{12}$$

The SOC of the supercapacitors at time k is calculated as

$$SOC_{sc}(k) = \frac{U_{sc}(k-1) - \frac{i_{sc}(k-1)}{C_{sc}(k-1)}}{U_{sc,max}} \tag{13}$$

To make sure the supercapacitors can recover the regenerative braking energy efficiently, the SOC of the supercapacitors is corrected according to the vehicle velocity during the driving process.

$$SOC_{sc}^*(k) = SOC_{sc,max}\sqrt{1 - \left(1 - \frac{U_{sc,min}^2}{U_{sc,max}^2}\right)\left(\frac{v(k)}{v_{max}}\right)^2} \tag{14}$$

where SOC^*sc is the corrected SOC, $SOC_{sc,max}$ is the maximum SOC, $U_{sc,max}$ and $U_{sc,min}$ are the maximum and minimum voltages of the supercapacitors, respectively, and v_{max} is the maximum vehicle velocity. The designed supercapacitor pack consists of Maxwell's 48-V module and the detailed parameters are obtained from a laboratory test.

The DC/DC model of the HESS uses a 2D map to determine the energy efficiency based on the input power and the voltage ratio, which can provide a good precision and a fast calculation speed.

4. Energy management strategy design

The control strategy of a coaxial power-split hybrid powertrain only using supercapacitors as energy storage system was designed by Ouyang et al. previously, which involves series hybrid mode, parallel hybrid mode, and the mode transition logic [28]. For the coaxial power-split hybrid powertrain with an HESS, one more task must be designed—the energy management strategy of the HESS. The thermostatic control, the power follower control, and the optimal control [29] are the three main control strategies for the series hybrid mode while the parallel electric assist control, the adaptive control, and the fuzzy logic control are normally used for the parallel hybrid mode. Currently, the rule-based control, the filter control, the model predictive control, and the fuzzy logic control are the four main control strategies of an HESS to distribute the power demand between the batteries and the supercapacitors.

Investigations indicate that the performance of rule-based control strategy can approach to that of the optimal control after optimization of the parameters of the rule-based control [30].

Therefore, in this study, a rule-based control strategy for the coaxial power-split hybrid powertrain is designed and is shown in **Figure 3**. The entire rule-based control strategy is composed of a series mode control and a parallel mode control as well as an HESS control. The series mode control strategy uses a power follower control method shown in **Figure 3**. If the driving power demand of the vehicle is lower than a certain value, the system enters the series mode control. First, the required power of the motor P_d is computed according to the system mathematical model. Then, the output power of the engine is determined based on the generator efficiency map. The modified discharging/charging power is calculated according to the difference between the present SOC and the target one. Subsequently, the requested power of the diesel engine is determined according to the defined optimal operation line (OOL) of the series mode control [31]. Meanwhile, the engine on/off state is decided due to the required power P_d and the current SOC. If the engine state is on, the final required engine torque and speed are computed according to the requested power of the engine and the defined OOL.
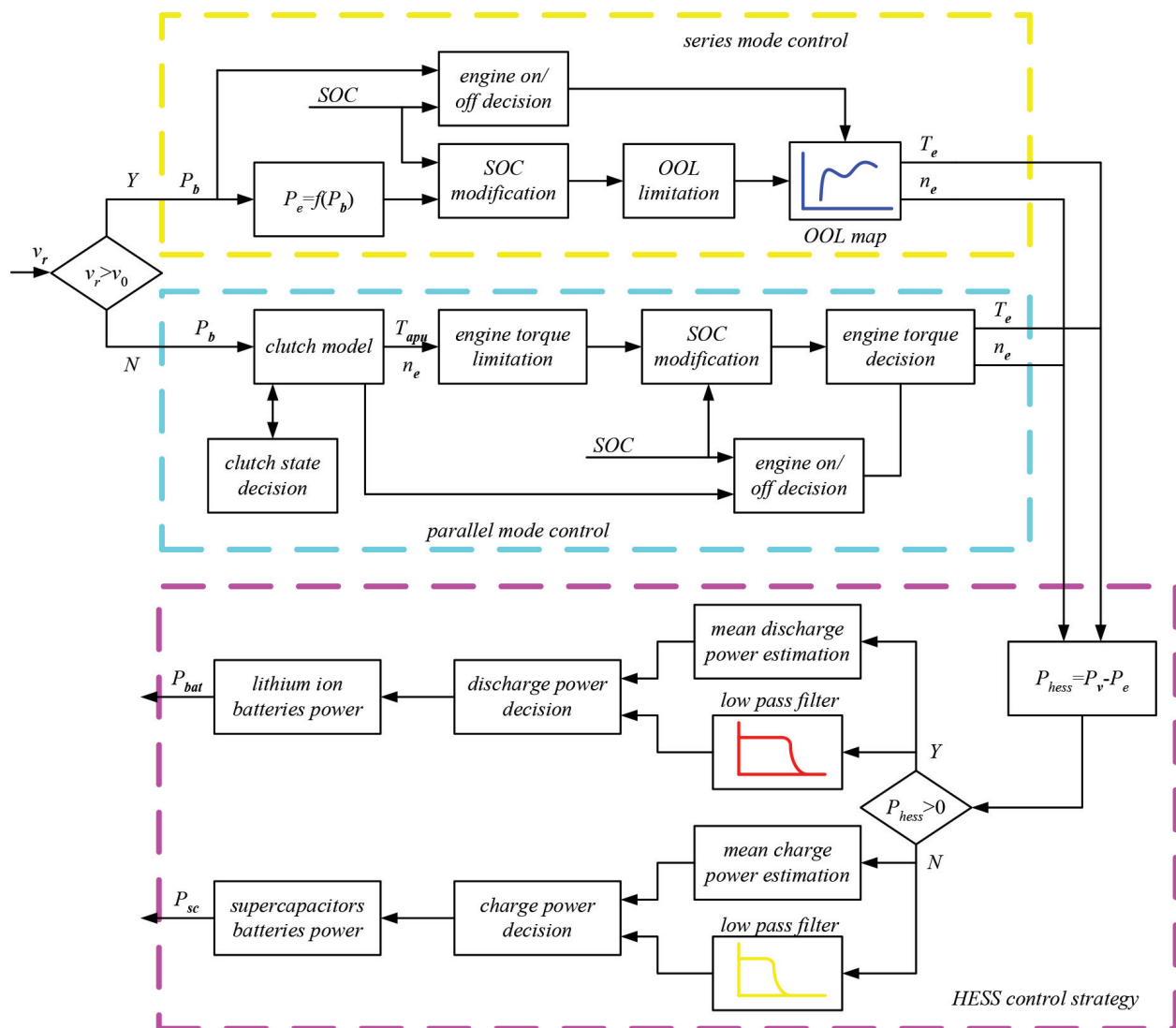
Figure 3. Control strategy for the coaxial power-split hybrid powertrain with an HESS composed of a series mode control and a parallel mode control as well as an HESS control strategy.

If the vehicle velocity is greater than the set value, the system changes to the parallel mode control. A parallel electric assist control strategy is used in this research and is shown in **Figure 3**. First, the demanded speed and torque of the auxiliary power unit are determined by the clutch model according to the power demand of the motor P_d. In the clutch model, the decision logic of the clutch state sets the working state of the clutch. When the clutch is engaged at the parallel mode control, the requested torque of the APU, which equals the output torque of the engine, is the summation of the driving torque directly transferred to the final drive and the charge torque that is transmitted to the generator. The motor provides the remaining driving torque simultaneously. Subsequently, the control parameters of the parallel mode are optimized across the overall engine's working region. Same as the series mode control, the modified discharging/charging power is calculated. Then, engine on/off state is decided by the clutch state and the SOC as well as the requested vehicle velocity. At last, the requested torque and speed of the engine are determined based on the engine state and the power demand.

The requested power of the diesel engine is obtained by the series or parallel control strategy. Then, the power demand of the HESS P_{hess} can be calculated as the difference between the power demand of the motor and the request power of the diesel engine. The HESS energy management strategy is in charge of the distribution of the power demand between the lithium-ion batteries and the supercapacitors. The detailed strategy shown in **Figure 3** is a combination of the rule-based control and the filter control. If P_{hess} is positive, the HESS should output electric power to the power line. First, an algorithm estimates the mean discharge power during the driving cycle and a low-pass filter outputs a filtered discharge power of the batteries. Then, the discharging power decision block calculates the output powers of the batteries and the supercapacitors based on the designed threshold values of SOC and the mean discharge power. If P_{hess} is negative, the motor outputs electric power to charge the HESS. Thereby, the control strategy is similar with the positive situation. Meanwhile, an SOC correction algorithm of the supercapacitors is employed based on the vehicle velocity for the discharging process.

5. Results and discussion

A program was developed using Matlab and Advisor according to the mathematical model of the coaxial power-split hybrid powertrain with an HESS. The designed simulation model combines the backward- and forward-facing methods and can evaluate the drivability and economy of the coaxial power-split hybrid powertrain system. In this research, a hybrid transit bus with a total mass of 15 ton manufactured by Higer Bus Company Limited is applied. The detailed parameters of the hybrid transit bus are listed in **Table 2**.

Using the CTBCDC driving cycle, the performance of the designed coaxial power-split hybrid powertrain with an HESS is evaluated, and the results are shown in **Figure 4**. The target and available values of the vehicle speed are compared in **Figure 4a**. The target vehicle speed is defined by the CTBCDC driving cycle. The available vehicle speed is determined using the established program and can follow the target one perfectly, which means the coaxial power-split hybrid powertrain with an HESS can satisfy the requirements of the drivability completely. The evaluated power demand of the motor is shown as the solid profile of **Figure 4b**. As a contrast, the output power of the diesel engine is given as the dashed line.

Parameter	Value	Unit
Vehicle mass excluding pack	12,930	kg
Cargo mass	2070	kg
Dimensions	$12 \times 2.55 \times 3$	m × m × m
Rolling resistance coefficient	0.0094	–
Aerodynamic drag coefficient	0.70	–
Vehicle frontal area	7.65	m^2
Wheel radius	0.506	m
Final gear	5.833	–

Table 2. Parameters of the transit bus.

The designed coaxial power-split hybrid powertrain with an HESS can recover the braking energy efficiently during the regenerative braking. When the vehicle is driving, the power demand of the motor increases with the vehicle velocity and the diesel engine will start and provide part of the driving energy if the driving power demand of the vehicle is greater than the specified value of the series mode control or the parallel mode control.

The system operation state is shown in **Figure 4c**, where 0 represents the EV mode, 1 means the series control mode, and 2 denotes the parallel control mode. If the vehicle driving power is greater than 110 kW, the operation mode switches from the series mode to the parallel mode. Meanwhile, the EV mode can be changed from both the series control mode and the parallel control mode. The output speed and torque of the diesel engine are shown in **Figure 4d** and **e**, respectively. Because the power follower control is used for the series control mode and the engine speed is proportional to the vehicle velocity at the parallel mode, the engine speed varied from 1494 to 1842 r/min during the working process. Furthermore, the engine output torque maintains at a high level of 550.4–761.6 Nm when the engine is running.

The performance of the HESS for the coaxial power-split hybrid powertrain is displayed in **Figure 5**. The output power of the HESS is given in **Figure 5a**. The output powers of each of the energy storage devices are given in **Figure 5b**, where the dashed line is used for the lithium-ion batteries, and the dash dotted line is used for the supercapacitors. In **Figure 5**, positive values represent discharging process and negative is used for charging. The output power of the HESS varies with the power demand of the motor. The maximum and minimum output powers achieve 104.8 and −112.9 kW, respectively. The output power of the lithium-ion batteries changes from −50 to 50 kW during the driving cycle, which means the output current of the batteries can be significantly decreased. The supercapacitors discharge or charge with large powers for the high-power working conditions to compensate the power difference between P_{hess} and P_{bat}. The SOC profiles for the lithium-ion batteries and the supercapacitors are shown in **Figure 6c**. During the charge sustain mode, the SOC of the batteries manifests a very small variation during the cycle. As a contrast, the SOC of the supercapacitors varies within a wide range from 0.395 to 0.99. The reason is that the capacity of the lithium-ion batteries is much greater than that of the supercapacitors and the output power of the lithium-ion batteries is constrained to a small range. The output voltages of the batteries and the supercapacitors are shown in **Figure 5d**. The output voltage of the lithium-ion batteries, which equals the power line voltage, changes in a very small
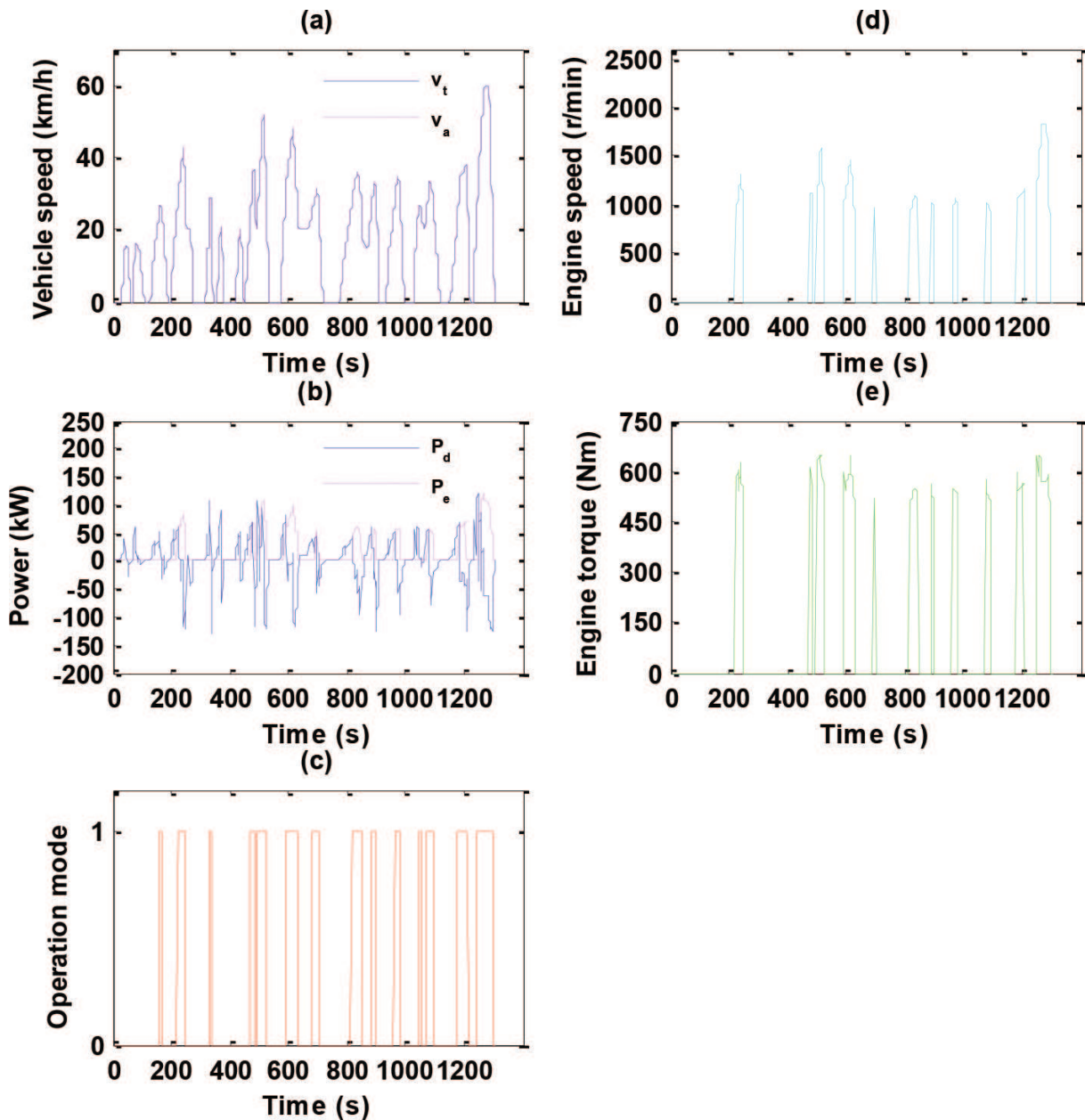
Figure 4. Analysis results of the system performance of the designed coaxial power-split hybrid powertrain with an HESS using the Chinese Transit Bus City Driving Cycle: (a) comparison of the target and estimated vehicle speeds, (b) the driving power requested by the transit bus P_d and the requested power provided by the engine P_e, (c) the system operation mode where 0 means pure electric vehicle mode and 1 represents series hybrid mode and 2 is parallel hybrid mode, (d) the engine speed, and (e) the engine requested torque.

range from 559.1 to 584.9 V. The stable voltage characteristic will be beneficial for the operations of the motor and the generator. Although the output voltage of the supercapacitors varies in a large scope, it is still within the allowable voltage ratio of the DC/DC module. The currents of the batteries and the supercapacitors are displayed in **Figure 5e**. The current of the supercapacitors increases while the current of the batteries is much smaller and the discharging/charging rate of the batteries is less than 4C, which is very helpful for the life extension of the batteries.
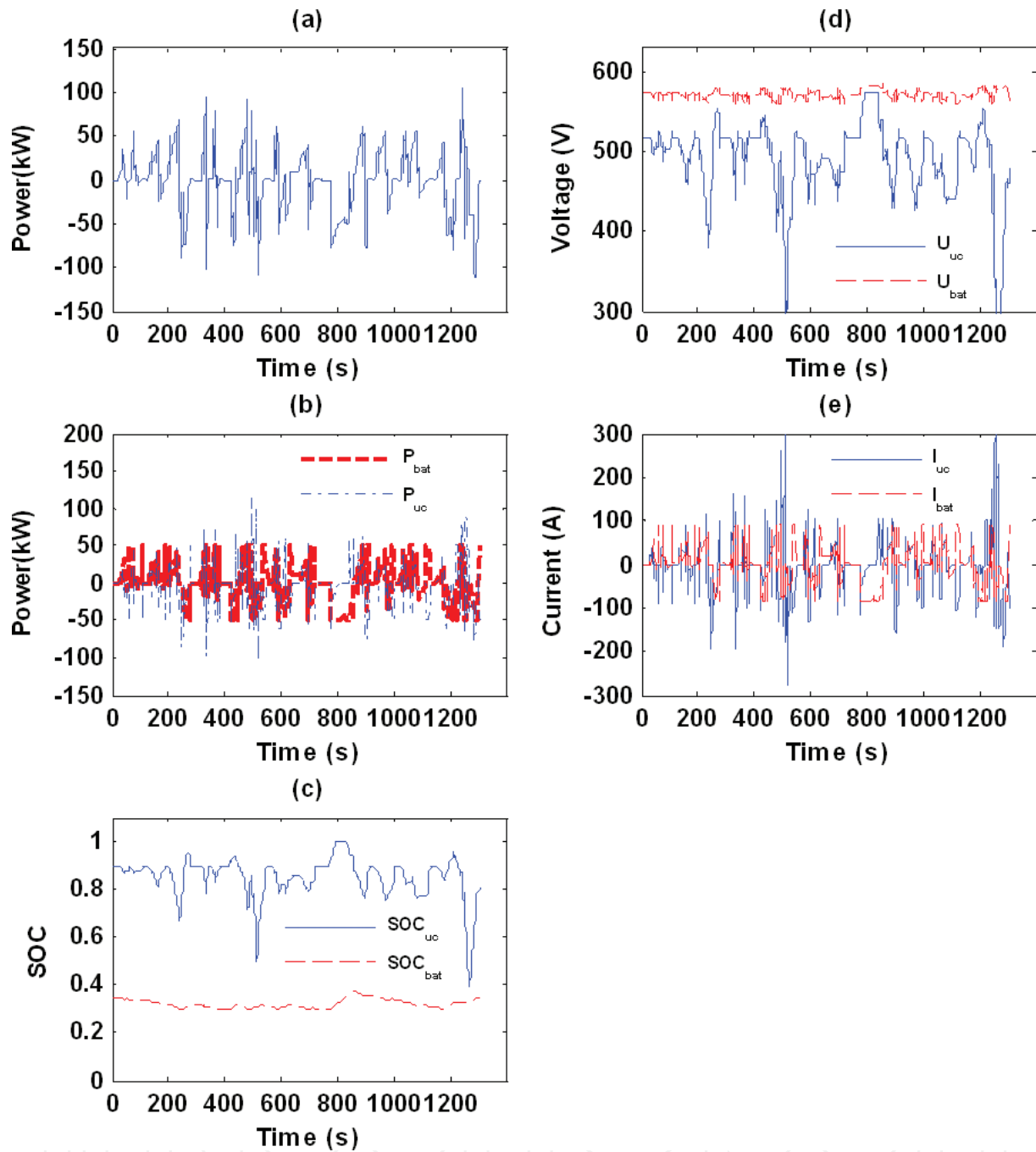
Figure 5. Analysis results for the performance of the HESS system: (a) the electric power output by the HESS, (b) the power outputs of the batteries P_{bat} and the supercapacitors P_{sc}, (c) SOCs of the batteries SOC_{bat} and the supercapacitors SOC_{sc}, (d) output voltages of the batteries U_{bat} and the supercapacitors U_{sc}, (e) output currents of the batteries i_{bat} and the supercapacitors i_{sc} where positive values denote discharging process and negative for charging.

Figure 6 gives the performances of the motor and the generator of the coaxial power-split hybrid powertrain with an HESS. The input power of the motor generally follows the vehicle driving power during the cycle, which means only a small part of the mechanical power of the diesel engine is used to propel the vehicle directly. Although the current of the motor varies in a wide range from −193.6 to 215.9 A, it does not exceed the maximum operation current of the motor.

The generator operates only a small part of the time and its output power changes mainly from 24.38 to 104.8 kW. The current of the generator varies with the output power because the power line voltage is stable.

To evaluate the potential of fuel saving for the coaxial power-split hybrid powertrain with an HESS, 12 prototypes of hybrid transit bus were built and applied to a practical city routes in Ningbo, Zhejiang Province. A total mileage of over 40,000 km for each hybrid transit bus was achieved, and the average fuel consumption is approximately 24.53 L/100 km, which is listed in **Table 3**. Using the established mathematical model and the analysis program, the estimated fuel consumption of the coaxial power-split hybrid powertrain with an HESS is 24.43 L/100 km, which is also listed in **Table 3**. The SOC difference of the lithium-ion batteries between the start and end points is 0.0034. The practical driving routes in Ningbo are different with the CTBCDC driving cycle. The start/stop frequency is decreased compared with the CTBCDC driving cycle. Therefore, the improvement of fuel efficiency is a bit lower. On the other hand, the ambient temperature and the total vehicle weight varying during the practical driving conditions also
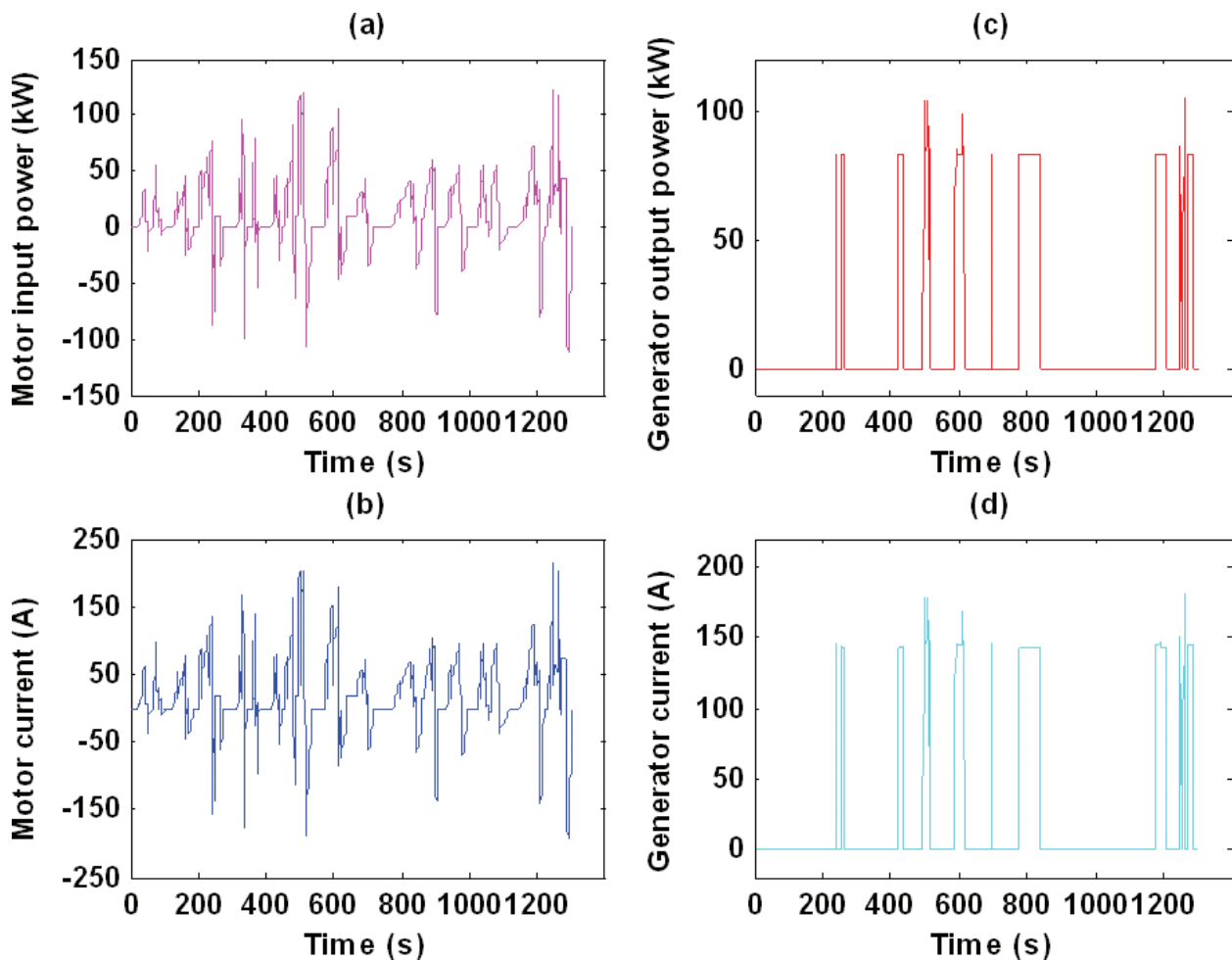
Figure 6. Results of the motor and the generator: (a) the input power of the motor (a positive value is used for driving process and a negative one is for regenerative braking), (b) the output current of the motor, (c) the requested power of the generator, and (d) the output current of the generator.

have a great influence on the fuel consumption. Herein, the experimental result only gives a very coarse and average evaluation of the fuel efficiency. Moreover, the fuel consumption of a conventional powertrain using a YC6G270 diesel engine and a five-gear manual transmission is computed based on the same vehicle parameters as the hybrid transit bus. The total mass of the bus with the conventional powertrain is 15,000 kg, which is the same as that of the coaxial power-split hybrid powertrain with an HESS. The result is 36.33 L/100 km. Compared with the results of the conventional powertrain, the fuel consumption of the coaxial power-split hybrid powertrain with an HESS can be decreased significantly by about 32.5%.

From the viewpoint of energy efficiency, the reason for such a great fuel reduction can be explained. **Figure 7** shows the effective thermal efficiency map of the YC6J220 diesel engine obtained on an engine test bench. The engine's working points estimated by the analysis program are also displayed. The OOL line of the series control mode is represented by the thick solid line in **Figure 7**. As a contrast, the effective thermal efficiency map of the YC6G270 diesel engine for the conventional powertrain and the corresponding working points are given in **Figure 8**. It can be seen that the engine working points of the coaxial power-split hybrid powertrain with an HESS are very close to the region having the peak efficiency and their thermal efficiencies are greater than 40%. However, the working points of the conventional powertrain shown in **Figure 8** will change with the vehicle velocity, resulting in a very wide distribution from the idle speed to the full load. Therefore, many working points of the conventional powertrain locate in the low-efficiency regions, leading to a low efficiency of the entire powertrain system.

The energy efficiency map of the PMSM obtained on a motor test bench and the relative working points for the CTBCDC driving cycle are given in **Figure 9**. A large part of the working points situates close to the peak-efficiency region. The efficiencies of most of the working points are higher than 93.4% except for the low-speed and small-load regions. The energy-weighted average efficiency of the motor during the CTBCDC driving cycle is 91.92%. Because the motor is connected to the final drive without a transmission, a particular design of the PMSM can ensure that the motor efficiency is high enough for low-speed working conditions. The energy efficiency map of the PMSG measured on a motor test bench and the corresponding working points for the CTBCDC driving cycle are displayed in **Figure 10**. The efficiencies of the PMSG are found to be between 92 and 93% during the CTBCDC driving cycle, and the energy-weighted average efficiency is 92.55%, which approaches the peak efficiency of the PMSG

Powertrain	Fuel consumption (l/100 km)	Energy reduction[a] (%)
Conventional powertrain bus	36.33	
Coaxial power-split hybrid bus	24.43[b]	32.76
	24.53[c]	32.48

[a]Relative to the conventional bus equipped with a YC6G270 diesel engine.
[b]Analysis result of the hybrid transit bus equipped with a YC6J220 diesel engine.
[c]Test result of the hybrid transit bus equipped with a YC6J220 diesel engine.
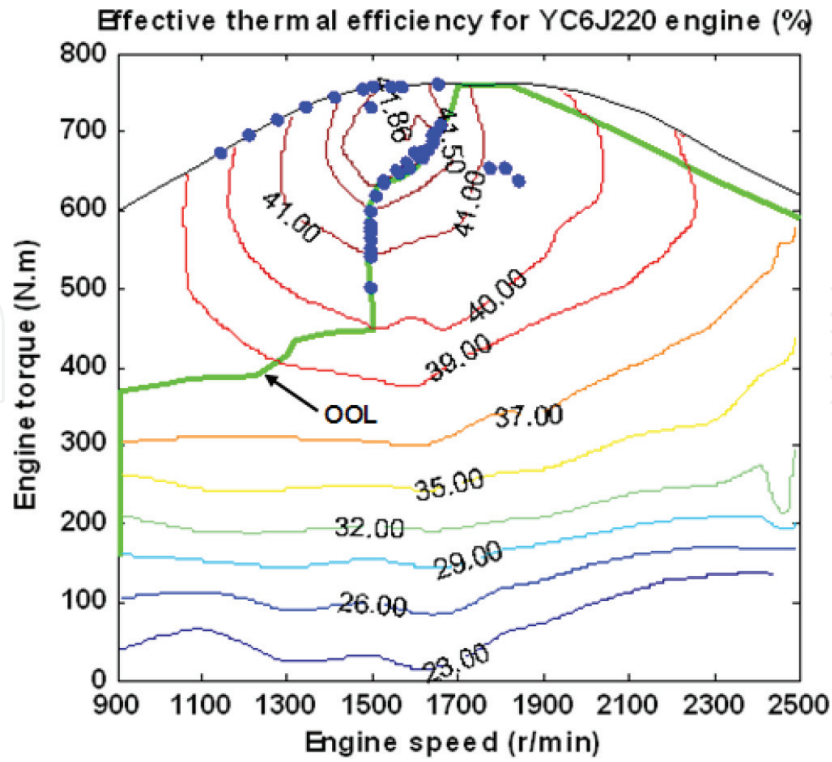
Table 3. Results of fuel consumption.

Figure 7. Energy efficiency map of the YC6J220 diesel engine measured on a test bench where the points denote the operation conditions of the diesel engine for the coaxial power-split hybrid powertrain with an HESS.
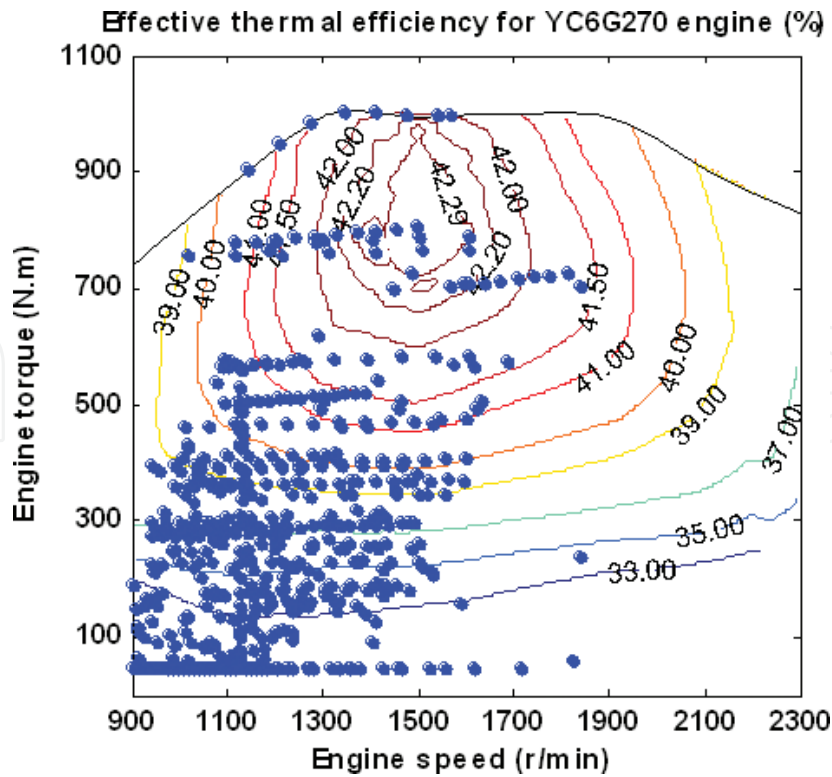

Figure 8. Analysis results of the conventional powertrain using a YC6G270 diesel engine and a five-gear transmission.
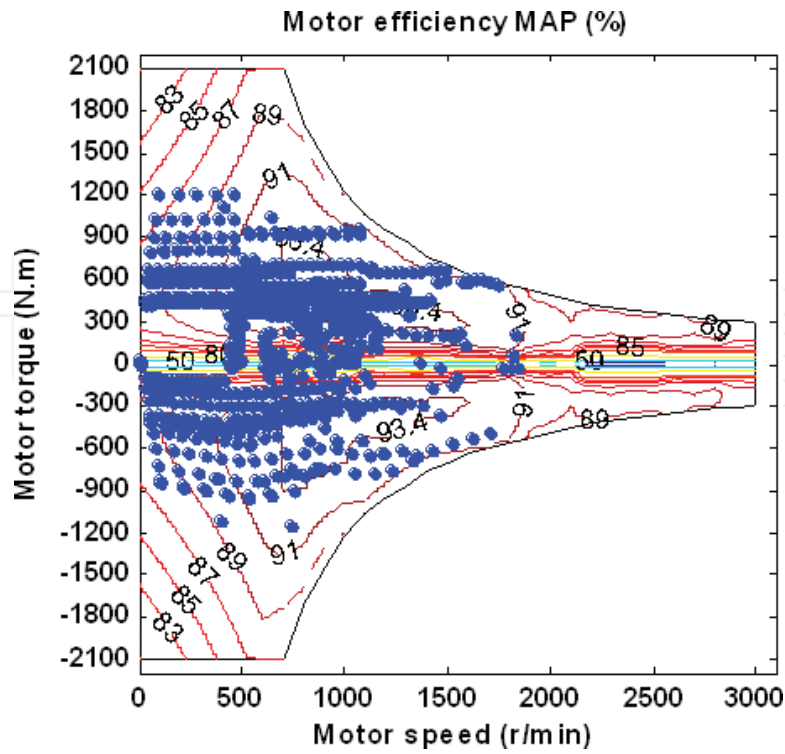
Figure 9. Energy efficiency map of the motor measured on a motor test bench where the points denote operation points of the motor for the coaxial power-split hybrid powertrain with an HESS.
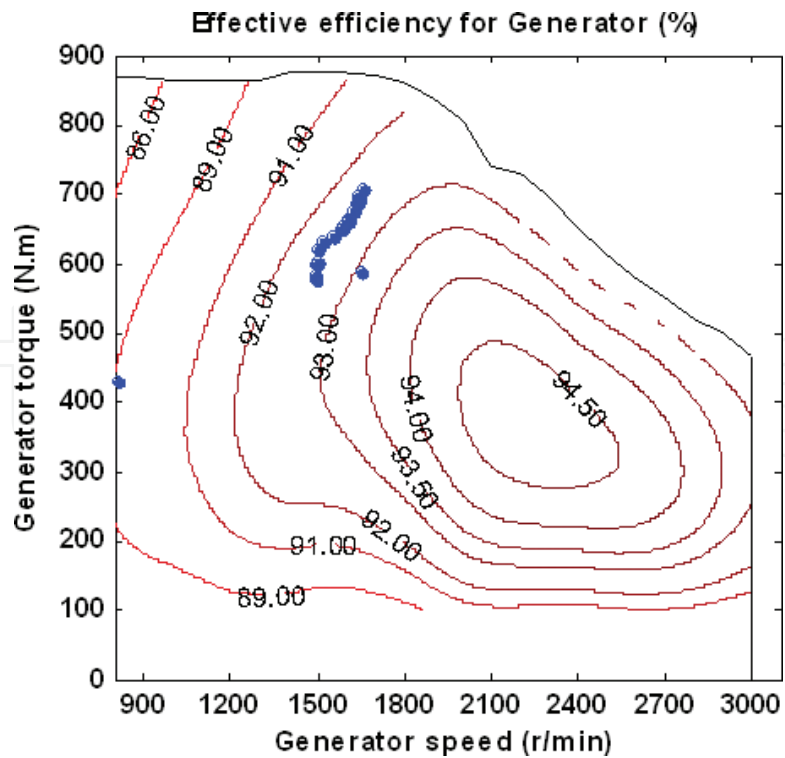

Figure 10. Energy efficiency map of the generator measured on a motor test bench where the points denote operation points of the generator for the coaxial power-split hybrid powertrain with an HESS.

6. Conclusions

In this study, the system performance of a coaxial power-split hybrid powertrain with an HESS for transit bus application was investigated. First, a system topology was designed. Then, a mathematical model was established and an energy management strategy was developed. Finally, the energy efficiency of the hybrid powertrain system was evaluated by Matlab and Advisor. The main conclusions are summarized as follows:

1. Compared with the results of a coaxial power-split hybrid powertrain with supercapacitors as energy storage device, the equivalent fuel consumption of the designed coaxial power-split hybrid powertrain with an HESS is a bit higher (24.43 vs. 20.46 L/100 km). The reason is that the energy capacity of the supercapacitors in this study is much smaller than that of the hybrid powertrain with only supercapacitors. Thus, the amount of the recovered regenerative energy is smaller than that of the hybrid powertrain with only supercapacitors. On the other hand, the DC/DC converter and the battery pack also have some losses during the working processes. As a result, the energy efficiency of the coaxial power-split hybrid powertrain with an HESS is lower than that of the hybrid powertrain with supercapacitors. Because we have no data about the coaxial power-split hybrid powertrain with only batteries, a quantitative comparison cannot be given here. Generally, if only batteries are used for the energy storage system, a large size will be used and the cost will increase a lot. The energy efficiency of such a system will be a trade-off between cost and lifetime of the batteries. Nevertheless, the results of this study show that the coaxial power-split hybrid powertrain with an HESS has a very good energy efficiency compared with a conventional powertrain of the same level.

2. Because the designed HESS has a smaller size and weight and lower price than that with only supercapacitors, and the lithium-ion batteries of the HESS can operate at an averaged current and thus have a longer life cycle, the HESS is more suitable for hybrid transit bus application.

3. The power line voltage of the HESS is more stable than that with only supercapacitors. This will be beneficial for the operation of the accessories such as the air conditioner or the in-vehicle infotainment system during the driving process.

Nomenclature

A vehicle frontal area (m^2)
C capacitance (F)
C_D aerodynamic drag coefficient
F tractive force (N)
f rolling resistance coefficient
g standard gravitational acceleration (9.8067 m/s^2)
i current (A)
J inertia (kg·m^2)

M fuel consumption (L/100 km)

m vehicle mass (kg)

P power (W)

R resistance (Ω)

T torque (Nm)

t time (s)

U voltage (V)

v vehicle velocity (m/s)

Greek letters

α road angle (°)

δ mass factor

ρ air density (kg/m^3)

ω angular speed of a tire

Subscript

0   final drive

a   aerodynamic

b   braking

bat   battery

e   engine

f   fuel

g   generator

i   grade resistance

j   acceleration

l   loss

m   motor

r   rolling, rear, reduced

sc   supercapacitor

w   wheel

Acronyms

APU   auxiliary power unit

CTBCDC   Chinese Transit Bus City Driving Cycle

ESS   energy storage system

EV   electric vehicle

FCV   fuel cell vehicle

HESS   hybrid energy storage system

HEV   hybrid electric vehicle
ICE   internal combustion engine
OOL   optimal operation line
PMSG   permanent magnetic synchronous generator
PMSM   permanent magnetic synchronous motor
SOC   state of charge

Author details

Enhua Wang[1], Fuyuan Yang[2] and Minggao Ouyang[2]*

*Address all correspondence to: ouymg@tsinghua.edu.cn

1 School of Mechanical Engineering, Beijing Institute of Technology, Beijing, China

2 State Key Laboratory of Automotive Safety and Energy, Tsinghua University, Beijing, China

References

[1] Kuhne R. Electric buses—An energy efficient urban transportation means. Energy. 2010;**35**:4510–4513.

[2] Chiara F, Canova M. A review of energy consumption, management, and recovery in automotive systems, with considerations of future trends. Proc I Mech Eng D-J Aut. 2013;**227**:914–936.

[3] Lajunen A. Energy consumption and cost-benefit analysis of hybrid and electric city buses. Transport Res C. 2014;**38**:1–15.

[4] Shen J, Dusmez S, Khaligh A. Optimization of sizing and battery cycle life in battery/ultracapacitor hybrid energy storage systems for electric vehicle applications. IEEE T Ind Electron. 2014;**10**:2112–2121.

[5] Capasso C, Veneri O. Experimental analysis on the performance of lithium based batteries for road full electric and hybrid vehicles. Appl Energ. 2014;**136**:921–930.

[6] Koohi-Kamali S, Tyagi VV, Rahim NA, Panwar NL, Mokhlis H. Emergence of energy storage technologies as the solution for reliable operation of smart power systems: A review. Renew Sust Energ Rev. 2013;**25**:135–165.

[7] Vangari M, Pryor T, Jiang L. Supercapacitors: Review of materials and fabrication methods. J Energy Eng. 2013;**139**:72–79.

[8] Zhang LL, Zhao XS. Carbon-based materials as supercapacitor electrodes. Chem Soc Rev. 2009;**38**:2520–2531.

[9] Yu Z, Duong B, Abbitt D, Thomas J. Highly ordered MnO_2 nanopillars for enhanced supercapacitor performance. Adv Mater. 2013;**25**:3302–3306.

[10] Gao Y, Zhou YS, Qian M, He XN, Redepenning J, Goodman P, Li HM, et al. Chemical activation of carbon nano-onions for high-rate supercapacitor electrodes. Carbon. 2013;**51**:52–58.

[11] Kuperman A, Aharon I. Battery–ultracapacitor hybrids for pulsed current loads: A review. Renew Sust Energ Rev. 2011;**15**:981–992.

[12] Cao J, Emadi A. A new battery/ultracapacitor hybrid energy storage system for electric, hybrid, and plug-in hybrid electric vehicles. IEEE T Power Electr. 2012;**27**:122–132.

[13] Song Z, Hofmann H, Li J, Han X, Zhang X, Ouyang M. A comparison study of different semi-active hybrid energy storage system topologies for electric vehicles. J Power Sources. 2015;**274**:400–411.

[14] Rothgang S, Baumhöfer T, van Hoek H, Lange T, De Doncker RW, Sauer DU. Modular battery design for reliable, flexible and multi-technology energy storage systems. Appl Energ. 2015;**137**:931–937.

[15] Hung YH, Wu CH. An integrated optimization approach for a hybrid energy system in electric vehicles. Appl Energ. 2012;**98**:479–490.

[16] Vulturescu B, Trigui R, Lallemand R, Coquery G. Implementation and test of a hybrid storage system on an electric urban bus. Transport Res C. 2013;**30**:55–66.

[17] Song Z, Hofmann H, Li J, Hou J, Han X, Ouyang M. Energy management strategies comparison for electric vehicles with hybrid energy storage system. Appl Energ. 2014;**134**:321–331.

[18] Yu Z, Zinger D, Bose A. An innovative optimal power allocation strategy for fuel cell, battery and supercapacitor hybrid electric vehicle. J Power Sources. 2011;**196**:2351–2359.

[19] Hu X, Johannesson L, Murgovski N, Egardt B. Longevity-conscious dimensioning and power management of the hybrid energy storage system in a fuel cell hybrid electric bus. Appl Energ. 2015;**137**:913–924.

[20] Paladini V, Donateo T, de Risi A, Laforgia D. Super-capacitors fuel-cell hybrid electric vehicle optimization and control strategy development. Energ Convers Manage. 2007;**48** (11):3001–3008.

[21] Masih-Tehrani M, Ha'iri-Yazdi MR, Esfahanian V, Safaei A. Optimum sizing and optimum energy management of a hybrid energy storage system for lithium battery life improvement. J Power Sources. 2013;**244**:2–10.

[22] Nguyen A, Lauber J, Dambrine M. Optimal control based algorithms for energy management of automotive power systems with battery/supercapacitor storage devices. Energ Convers Manage. 2014;**87**:410–420.

[23] Ehsani M, Gao Y, Emadi A. Modern electric, hybrid electric, and fuel cell vehicles: Fundamentals, theory, and design. 2nd ed. New York, NY: CRC Press; 2009.

[24] Advisor version 2003. Advisor help documentation. US: National Renewable Energy Laboratory; 2013.

[25] Bataus M, Maciac A, Oprean M, Vasiliu N. Automotive clutch models for real time simulation. Proc Romanian Acad A. 2011;**12**:109–116.

[26] Malik A, Zhang Z, Agarwal RK. Extraction of battery parameters using a multi-objective genetic algorithm with a non-linear circuit model. J Power Sources. 2014;**259**:76–86.

[27] A123 datasheet of 26650m1b. US: A123 Systems Inc.; 2012.

[28] Ouyang M, Zhang W, Wang E, Yang F, Li J, Li Z, Yu P, Ye X. Performance analysis of a novel coaxial power-split hybrid powertrain using a CNG engine and supercapacitors. Appl Energ. 2015;**157**:595–606.

[29] Sorrentino M, Rizzo G, Arsie I. Analysis of a rule-based control strategy for on-board energy management of series hybrid vehicles. Control Eng Pract. 2011;**19**:1433–1441.

[30] Vinot E, Trigui R. Optimal energy management of HEVs with hybrid storage system. Energ Convers Manage. 2013;**76**:437–452.

[31] Kim N, Cha S, Peng H. Optimal control of hybrid electric vehicles based on Pontryagin's minimum principle. IEEE T Veh Technol. 2011;**19**:1279–1287.